Four-Dimensional Computed Tomography Evaluation of Shoulder Joint Motion in Collegiate Baseball Pitchers

Daisuke Momma (d-momma@med.hokudai.ac.jp)
Hokkaido University Hospital
Alejandro A Espinoza Orías
Rush University Medical Center
Tohru Irie
Hokkaido University
Tomoyo Irie
Hokkaido University
Eiji Kondo
Hokkaido University Hospital
Norimasa Iwasaki
Hokkaido University
Nozomu Inoue
Rush University Medical Center

Research Article

Keywords: glenohumeral contact area, four-dimensional computed tomography (4D CT), cocking motion, micromotion

Posted Date: June 29th, 2021

DOI: https://doi.org/10.21203/rs.3.rs-648232/v1

Version of Record: A version of this preprint was published at Scientific Reports on February 25th, 2022.
See the published version at https://doi.org/10.1038/s41598-022-06464-5.

Abstract

The purpose of this study is to evaluate the glenohumeral contact area, center of glenohumeral contact area, and center of humeral head during simulated pitching motion in collegiate baseball pitchers using four-dimensional computed tomography (4D CT). We obtained 4D CT data from the dominant and non-dominant shoulders of eight collegiate baseball pitchers during the cocking motion. CT image data of each joint were reconstructed using a 3D reconstruction software package. The glenohumeral contact area, center of glenohumeral contact area, center of humeral head, and oblateness of humeral head were calculated from 3D bone models using customized software. The center of glenohumeral contact area translated significantly from anterior to posterior during maximum external rotation to maximum internal rotation. The center of humeral head translated from posterior to anterior during maximum external rotation to maximum internal rotation. There was a high negative correlation between anterior translation of the center of glenohumeral contact area and center of humeral head, and a positive correlation between the translation and the oblateness. 4D CT analyses demonstrated that the center of humeral head translated in the opposite direction to that of the center of glenohumeral contact area during external rotation to internal rotation in abduction in the dominant and non-dominant shoulders. This diametric translation can be explained by the oblateness of the humeral head. 4D CT scanning and the software for bone surface modeling of the glenohumeral joint enabled quantitative assessment of glenohumeral micromotion and identified humeral head oblateness as the cause of diametric change.

Introduction

Glenohumeral joint micromotion and shoulder internal impingement are the important factors of shoulder pathology in throwing athletes. Pitching in baseball has been described as six discrete phases: wind up, stride, cocking, acceleration, deceleration, and follow through[1]. The cocking and acceleration phases are most commonly implicated in shoulder pathology of throwing, due to excessive abduction and external rotation of the glenohumeral joint[2]. Numerous studies have conducted overhead throwing analysis[3–6], but *in vivo* glenohumeral joint kinematics during pitching motion remains controversial because it is difficult to directly assess micromotion of the glenohumeral joint[7,8].

Glenohumeral joint contact patterns well reflect pathological conditions such as rotator cuff tear and glenohumeral joint instability[9,10]. Based on this theory, Bey et al. reported that joint contact patterns are not only a more sensitive measurement than conventional kinematics for detecting subtle differences in joint function but may also provide a more clinically relevant indication of the extent to which a conservative or surgical procedure has adequately restored normal joint function[11]. Therefore, measurement of glenohumeral joint contact patterns can reveal the kinematics of the glenohumeral joint in baseball players.

Measurement of glenohumeral joint mechanics is a challenging task, especially under *in vivo* conditions. The glenohumeral joint kinematics of normal shoulders have been evaluated using cadaveric specimens[12], radiographs[13], fluoroscopy[14], magnetic resonance imaging[15,16], and electromagnetic

tracking devices[17]. However, there are limitations associated with these conventional measuring techniques. In particular, cadaveric studies cannot accurately simulate *in vivo* conditions because the muscle forces and joint forces are unknown. Four-dimensional computed tomography (4D CT) enables these issues to be overcome, and can be used for the clinical evaluation in various fields, with a low radiation dose[18]. Previous studies have shown the potential of dynamic assessment with 4D CT technology for assessing complex pathologies and their underlying mechanisms[19,20]. We hypothesized that glenohumeral joint kinematics during simulated pitching motion could be quantitatively analyzed *in vivo* using a 4D CT device. The purpose of this study was to evaluate the glenohumeral contact area, center of glenohumeral contact area, and center of humeral head during simulated pitching motion in baseball players by 4D CT analysis.

Results

Participant demographics

4D CT imaging of both shoulders was performed in 8 male college volunteers (age, 18.6 ± 0.5 years; range, 18–19 years). There was no significant difference in the mean first ER or second IR between the dominant and non-dominant sides (Table 1). Mean second ER was significantly greater on the dominant side than on the non-dominant side ($p = .0179$).

Joint contact area

There was no significant difference in mean glenohumeral contact area between the dominant and non-dominant sides (Fig. 1). There was no significant difference in mean glenohumeral contact area during glenohumeral joint rotation: the mean value at maximum external rotation was 692.4 ± 96.2 mm^2 and 663.5 ± 69.2 mm^2, and the mean value at maximum internal rotation was 663.2 ± 115.4 mm^2 and 656.4 ± 101.3 mm^2, for the dominant and non-dominant sides, respectively. The mean value at midpoint from maximum external rotation to maximum internal rotation was 663.7 ± 107.6 mm^2 and 654.2 ± 89.5 mm^2, and the mean value at midpoint from maximum internal rotation to maximum external rotation was 659.5 ± 117.4 mm^2 and 649.7 ± 80.8 mm^2, for the dominant and non-dominant sides, respectively.

Figure 2A and B shows translation of the center of glenohumeral contact area from the original position during simulated pitching motion. On both the dominant and non-dominant sides, translation of the center of glenohumeral contact area increased gradually until maximum internal rotation, and then decreased to the point of maximum external rotation. On the dominant side, translation of the center of glenohumeral contact area from the original position was 0.85 ± 0.64 mm to the first maximum internal rotation and 0.89 ± 0.44 mm to the second maximum internal rotation. The same trend was observed on the non-dominant side, where translation of the center of glenohumeral contact area was 1.12 ± 0.68 mm from the original position to the first maximum internal rotation and 1.04 ± 0.59 mm to second maximum internal rotation was. There was no significant difference between the dominant and non-dominant sides in terms of change in the translation of the center of glenohumeral contact area.

When the translation was decomposed into superior, anterior, and medial directions (Fig. 3A-C), the direction toward superior and inferior translation was stable during glenohumeral joint rotation (Fig. 3A). Translation in the medial and lateral direction was also stable (Fig. 3C). That toward anterior and posterior directions was more changeable, and gradually translated posteriorly from the original position to maximum internal rotation (Fig. 3B). The posterior translation of the center of glenohumeral contact area from the original position to the first maximum internal rotation was 0.58 ± 0.63 mm on the dominant side (Fig. 3B). The same trend was observed on the non-dominant side, where posterior translation of the center of glenohumeral contact area from the original position to the first maximum internal rotation was 0.99 ± 0.82 mm (Fig. 3B).

Center of humeral head

The translations of the center of humeral head from the original position to all other positions are shown in Fig. 4A and B. On both the dominant and non-dominant sides, translation of the center of humeral head increased gradually until maximum internal rotation, and then decreased to the point of maximum external rotation. On the dominant side, translation of the center of humeral head from the original position was 1.20 ± 0.32 mm to the first maximum internal rotation, which was significantly higher than that to the first maximum external rotation (0.40 ± 0.18 mm, p = .0001) and that to the second maximum external rotation (0.45 ± 0.22 mm, p = .0003). Translation of the center of humeral head from the original position was 1.07 ± 0.35 mm to the second maximum internal rotation, which was significantly higher than that to the first maximum external rotation (p = .0024) and to the second maximum external rotation (p = .0059). Translation of the center of humeral head from the original position to the first midpoint of maximum external rotation to internal rotation (0.97 ± 0.39 mm) was significantly higher than that to the first maximum external rotation (p = .0141) and to the second maximum external rotation (p = .0316) (Fig. 4A). The same trend was observed on the non-dominant side, where translation of the center of humeral head from the original position was 1.47 ± 0.58 mm to the first maximum internal rotation, which was significantly higher than that to the first maximum external rotation (0.50 ± 0.35 mm, p = .0250) and that to the second maximum external rotation (0.34 ± 0.13 mm, p = .0050). Translation of the center of humeral head from the original position was 1.32 ± 0.82 mm to the second maximum internal rotation, which was significantly higher than that to the second maximum external rotation (p = .0241) (Fig. 4B).

When the translation was decomposed into superior, anterior, and medial directions (Fig. 5A-C), the direction toward superior and inferior translation was stable during glenohumeral joint rotation. Translation in the medial and lateral directions was also stable (Fig. 5C). That toward anterior and posterior directions was more changeable, and gradually translated anteriorly from the original position to maximum internal rotation (Fig. 5B). The anterior translation of the center of humeral head from the original position to the first maximum internal rotation was 0.76 ± 0.75 mm on the dominant side (Fig. 5B). The same trend was observed on the non-dominant side, where anterior translation of the center of humeral head from the original position to the first maximum internal rotation was 1.21 ± 0.78 mm (Fig. 5B).

Correlation between the center of glenohumeral contact area and the center of humeral head

A high positive correlation was found between the distance of center of glenohumeral contact area and the center of humeral head (dominant, r = 0.9763; non-dominant, r = 0.9535). There was no correlation between the superior translation of center of glenohumeral contact area and the center of humeral head (dominant, r = -0.0914; non-dominant, r = -0.3180). There was no correlation between the medial translation of the center of glenohumeral contact area and the center of humeral head (dominant, r = -0.3287; non-dominant, r = 0.0874). A high negative correlation was found between the anterior translation of the center of glenohumeral contact area and the center of humeral head (dominant, r = -0.7855; non-dominant, r = -0.7552).

Correlation between translation the center of humeral head and humeral head oblateness

A high positive correlation was found between the translation of the center of humeral head and humeral head oblateness (dominant, r = 0.6530; non-dominant, r = 0.6781).

Discussion

To the best of our knowledge, this is the first study to evaluate 4D alteration in glenohumeral contact area and translation of the center of humeral head during active cocking motion *in vivo*. The present findings demonstrated that the glenohumeral contact area altered during active cocking motion. In addition, the center of humeral head translated anteriorly during active abduction/internal rotation and posteriorly during active external rotation in abduction on both of the dominant and non-dominant sides.

Recent studies have demonstrated that glenohumeral contact area varies depending on the shoulder position. In a study of cadaveric shoulders, Greis[21] et al. reported that glenohumeral contact area increased 5.0% from 30° of abduction and neutral position to 90° abduction and neutral position. Bhatia[22] et al. reported that glenohumeral contact area decreased from 5.44 cm^2 in 60° of abduction and neutral position to 4.05 cm^2 in 60° abduction and 90° external rotation. However, most of these measurements were obtained in a series of static poses. Because internal forces differ between static and dynamic tasks, and the muscular pattern affects the glenohumeral contact area, we developed a protocol based on 4D CT and a customized computer program to measure 3D glenohumeral kinematics in dynamic motion. Recent developments have enabled multidetector CT scanners with wide CT gantries to obtain multiple scans in 0.1 s, and thus 4D CT analysis of joint motion[23,24]. We used this technology to evaluate the glenohumeral contact area quantitatively during active cocking motion with the shoulder abducted in baseball pitchers. The glenohumeral contact area in these intact shoulders tended to decreased during active abduction–internal rotation, but the change in glenohumeral contact area during dynamic motion was not statistically significant. The present results might be affected by the internal forces.

Excessive anterior translation of the humeral head during the throwing motion is thought to increase the risk of injury[25,26]. Glenohumeral translations has been a controversial topic as the range in reported values has been only a few millimeters below the limits of accuracy[27]. Furthermore, a previous study has reported that the center of humeral head translated 3.4 mm posteriorly during glenohumeral external rotation with the shoulder in the abduction[20]. The results of the present study found that the center of humeral head translated 1.20 ± 0.32 mm anteriorly during the cocking motion. Regarding the direction of humeral head translation, the current results are comparable to those of previous reports.

The current study showed that the center of the glenohumeral joint contact area translated posteriorly during shoulder internal rotation, whereas the center of humeral head translated anteriorly. This diametric translation appears to be caused by oblateness of the humeral head (Fig. 6). The current study hound a positive correlation between oblateness and translation of the center of humeral head. This result indicates diametric translation of the center of glenohumeral contact area and the center of humeral head.

There are some limitations of the present study. First, we did not image the entire scapula and humerus. Second, we used a surface registration technique. Finally, our analysis was not based on direct measurement of pitching motion; however, the shoulders consistently showed a characteristic pattern of glenohumeral kinematic changes, and the present results appear to accurately represent the glenohumeral kinematics of normal shoulders in the cocking motion.

In conclusion, 4D CT scanning and the tracer software for bone surface modeling of the glenohumeral joint show promise for evaluation of glenohumeral micromotion.

Methods

Ethics statement.

Our study was carried out in accordance with relevant guidelines of Hokkaido University Hospital and approved by the Research Ethics Review Committee of Hokkaido University Hospital. Our research protocols for human samples used in this study was approved by the Research Ethics Review Committee of Hokkaido University Hospital (approval ID: 011–0327). Informed consents for the use of samples in our research were obtained from all participants and their guardians. Informed consents for publication of identifying images in an online open-access publication were also obtained.

Subjects

We obtained 4D CT images of the dominant and non-dominant shoulders of eight baseball players as they performed the cocking motion. The participants were all male, without a history of shoulder complaints, with normal shoulder examination with no pain on shoulder joint palpation, and negative subacromial impingement test results. Body weight and height were recorded, and the shoulder range of motion was measured using a goniometer.

4D CT image data acquisition

All images were obtained with a 320-slice multidetector 4D CT scanner (Aquilion One; Toshiba Medical Systems, Tochigi, Japan) with a wide field-of-view (FOV), 0.5-mm slice thickness, and gantry tilt of 22°. The angle between the board and the ground was 27° (Fig. 7A). CT images were obtained with shoulder abduction of 90° and elbow flexion of 90°. The scan parameters were set as follows: dynamic volume scan; wide FOV (size, LL; detector width, 16 cm); 80 kV; 100 mA; gantry speed, 0.275 s/rotation; effective mAs, 27; reconstruction function, FC01; reconstruction rate, 0.1 s (31 volume); AIDR, standard; slice thickness, 0.5 mm; and slice interval, 0.5 mm. The scanning time was 3.3 s for two cocking motions controlled to a rhythm of 80 beats/min with a metronome. The total radiation exposure was set not to exceed 2.4 mSv.

Analysis of dynamic motion of glenohumeral joint

CT image data of each shoulder joint were imported in DICOM format and segmented using a segmentation software package (Mimics 21R; Materialise, Leuven, Belgium). Images were reconstructed to 3D scapula and humerus bone models, and the resulting 3D models were then exported as pointcloud and polygon models using the same software package. These 3D scapula and humerus bone models were then analyzed with a customized software created in Microsoft Visual C + + with Microsoft Foundation Class programming environment (Microsoft, Redmond, WA) for further analysis[28,29]. The glenohumeral contact area, center of glenohumeral contact area, and center of humeral head were analyzed with a customized software[30]. The major and minor axes of humeral head were also analyzed with a customized software. Oblateness of humeral head was defined as (major axis – minor axis) / major axis. The original position was defined as the first frame of maximum external rotation (MER) (Fig. 7B). A validated 3D-3D registration method was used to evaluate the translation of center of glenohumeral contact area and center of humeral head, and a transformation matrix from the original position to the rotated position was obtained[28,29]. We used International Society of Biomechanics standard as the anatomical coordinate system for the shoulder[31] (Fig. 8).

Statistical Analysis

We compared the glenohumeral contact area, oblateness of humeral head, translation of center of glenohumeral contact area, and translation of center of humeral head between the dominant and non-dominant sides using paired t test. One-way repeated-measures analysis of variance was used to investigate change in the glenohumeral contact area, translation of center of glenohumeral contact area, and center of humeral head per frame, The correlation between the translation of center of glenohumeral contact area and center of humeral head was examined. The correlation between the translation of center and humeral head oblateness was also examined. P values < .05 were considered significant. Data are presented as the mean ± SD and corresponding 95% confidence intervals.

Declarations

Author contributions

DM participated in the design of the study and carried out the experiments and statistical analysis. DM drafted the manuscript. AO, TI, TI, and NI assisted in carrying out the experiments and with the manuscript preparation. EK, and NI conceived of the study and provided assistance.

Conflict of interest: Non

Funding: Non

References

1. Fleisig, G. S., Barrentine, S. W., Zheng, N., Escamilla, R. F. & Andrews, J. R. Kinematic and kinetic comparison of baseball pitching among various levels of development. J Biomech 32, 1371-1375, doi:10.1016/s0021-9290(99)00127-x (1999).
2. Dillman, C. J., Fleisig, G. S. & Andrews, J. R. Biomechanics of pitching with emphasis upon shoulder kinematics. J Orthop Sports Phys Ther 18, 402-408, doi:10.2519/jospt.1993.18.2.402 (1993).
3. Glousman, R. et al. Dynamic electromyographic analysis of the throwing shoulder with glenohumeral instability. J Bone Joint Surg Am 70, 220-226 (1988).
4. Jobe, F. W., Tibone, J. E., Perry, J. & Moynes, D. An EMG analysis of the shoulder in throwing and pitching. A preliminary report. Am J Sports Med 11, 3-5, doi:10.1177/036354658301100102 (1983).
5. Lin, H. T. et al. Use of virtual, interactive, musculoskeletal system (VIMS) in modeling and analysis of shoulder throwing activity. J Biomech Eng 127, 525-530, doi:10.1115/1.1894387 (2005).
6. Davis, J. T. et al. The effect of pitching biomechanics on the upper extremity in youth and adolescent baseball pitchers. Am J Sports Med 37, 1484-1491, doi:10.1177/0363546509340226 (2009).
7. Fleisig, G. S. et al. Kinetic comparison among the fastball, curveball, change-up, and slider in collegiate baseball pitchers. Am J Sports Med 34, 423-430, doi:10.1177/0363546505280431 (2006).
8. Shimizu, T., Iwasaki, N., Nishida, K., Minami, A. & Funakoshi, T. Glenoid stress distribution in baseball players using computed tomography osteoabsorptiometry: a pilot study. Clin Orthop Relat Res 470, 1534-1539, doi:10.1007/s11999-012-2256-0 (2012).
9. Soslowsky, L. J. et al. Quantitation of in situ contact areas at the glenohumeral joint: a biomechanical study. J Orthop Res 10, 524-534, doi:10.1002/jor.1100100407 (1992).
10. Bey, M. J., Kline, S. K., Zauel, R., Kolowich, P. A. & Lock, T. R. In Vivo Measurement of Glenohumeral Joint Contact Patterns. EURASIP J Adv Signal Process 2010, doi:10.1155/2010/162136 (2010).
11. Bey, M. J. et al. In vivo shoulder function after surgical repair of a torn rotator cuff: glenohumeral joint mechanics, shoulder strength, clinical outcomes, and their interaction. Am J Sports Med 39, 2117-2129, doi:10.1177/0363546511412164 (2011).
12. Mihata, T. et al. Effect of scapular orientation on shoulder internal impingement in a cadaveric model of the cocking phase of throwing. J Bone Joint Surg Am 94, 1576-1583, doi:10.2106/JBJS.J.01972

(2012).

13. Howell, S. M., Galinat, B. J., Renzi, A. J. & Marone, P. J. Normal and abnormal mechanics of the glenohumeral joint in the horizontal plane. J Bone Joint Surg Am 70, 227-232 (1988).
14. Maki, N. J. Cineradiographic studies with shoulder instabilities. Am J Sports Med 16, 362-364, doi:10.1177/036354658801600410 (1988).
15. Di Giacomo, G. et al. Glenohumeral translation in ABER position during muscle activity in patients treated with Latarjet procedure: an in vivo MRI study. Knee Surg Sports Traumatol Arthrosc 24, 521-525, doi:10.1007/s00167-015-3896-x (2016).
16. von Eisenhart-Rothe, R. M., Jager, A., Englmeier, K. H., Vogl, T. J. & Graichen, H. Relevance of arm position and muscle activity on three-dimensional glenohumeral translation in patients with traumatic and atraumatic shoulder instability. Am J Sports Med 30, 514-522, doi:10.1177/03635465020300041101 (2002).
17. Lippitt, S. B., Harris, S. L., Harryman, D. T., 2nd, Sidles, J. & Matsen, F. A., 3rd. In vivo quantification of the laxity of normal and unstable glenohumeral joints. J Shoulder Elbow Surg 3, 215-223, doi:10.1016/S1058-2746(09)80038-4 (1994).
18. Edirisinghe, Y., Troupis, J. M., Patel, M., Smith, J. & Crossett, M. Dynamic motion analysis of dart throwers motion visualized through computerized tomography and calculation of the axis of rotation. J Hand Surg Eur Vol 39, 364-372, doi:10.1177/1753193413508709 (2014).
19. Alta, T. D., Bell, S. N., Troupis, J. M., Coghlan, J. A. & Miller, D. The new 4-dimensional computed tomographic scanner allows dynamic visualization and measurement of normal acromioclavicular joint motion in an unloaded and loaded condition. J Comput Assist Tomogr 36, 749-754, doi:10.1097/RCT.0b013e31826dbc50 (2012).
20. Matsumura, N. et al. Glenohumeral translation during active external rotation with the shoulder abducted in cases with glenohumeral instability: a 4-dimensional computed tomography analysis. J Shoulder Elbow Surg 28, 1903-1910, doi:10.1016/j.jse.2019.03.008 (2019).
21. Greis, P. E., Scuderi, M. G., Mohr, A., Bachus, K. N. & Burks, R. T. Glenohumeral articular contact areas and pressures following labral and osseous injury to the anteroinferior quadrant of the glenoid. J Shoulder Elbow Surg 11, 442-451, doi:10.1067/mse.2002.124526 (2002).
22. Bhatia, S. et al. Comparison of glenohumeral contact pressures and contact areas after glenoid reconstruction with latarjet or distal tibial osteochondral allografts. Am J Sports Med 41, 1900-1908, doi:10.1177/0363546513490646 (2013).
23. Hislop-Jambrich, J. L., Troupis, J. M. & Moaveni, A. K. The Use of a Dynamic 4-Dimensional Computed Tomography Scan in the Diagnosis of Atraumatic Posterior Sternoclavicular Joint Instability. J Comput Assist Tomogr 40, 576-577, doi:10.1097/RCT.0000000000000410 (2016).
24. Gobbi, R. G. et al. Patellar tracking after isolated medial patellofemoral ligament reconstruction: dynamic evaluation using computed tomography. Knee Surg Sports Traumatol Arthrosc 25, 3197-3205, doi:10.1007/s00167-016-4284-x (2017).

25. Akeda, M. et al. Lower shoulder abduction during throwing motion may cause forceful internal impingement and decreased anterior stability. J Shoulder Elbow Surg 27, 1125-1132, doi:10.1016/j.jse.2017.12.029 (2018).
26. Jobe, F. W., Giangarra, C. E., Kvitne, R. S. & Glousman, R. E. Anterior capsulolabral reconstruction of the shoulder in athletes in overhand sports. Am J Sports Med 19, 428-434, doi:10.1177/036354659101900502 (1991).
27. Veeger, H. E. & van der Helm, F. C. Shoulder function: the perfect compromise between mobility and stability. J Biomech 40, 2119-2129, doi:10.1016/j.jbiomech.2006.10.016 (2007).
28. Forsythe, B. et al. Dynamic 3-Dimensional Mapping of Isometric Anterior Cruciate Ligament Attachment Sites on the Tibia and Femur: Is Anatomic Also Isometric? Arthroscopy 34, 2466-2475, doi:10.1016/j.arthro.2018.03.033 (2018).
29. Forsythe, B. et al. Dynamic Three-Dimensional Computed Tomography Mapping of Isometric Posterior Cruciate Ligament Attachment Sites on the Tibia and Femur: Single vs Double Bundle Analysis. Arthroscopy, doi:10.1016/j.arthro.2020.06.006 (2020).
30. Yanke, A. B. et al. Sex Differences in Patients With CAM Deformities With Femoroacetabular Impingement: 3-Dimensional Computed Tomographic Quantification. Arthroscopy 31, 2301-2306, doi:10.1016/j.arthro.2015.06.007 (2015).
31. Wu, G. et al. ISB recommendation on definitions of joint coordinate systems of various joints for the reporting of human joint motion--Part II: shoulder, elbow, wrist and hand. J Biomech 38, 981-992, doi:10.1016/j.jbiomech.2004.05.042 (2005).

Tables

Due to technical limitations, tables are only available as a download in the Supplemental Files section.

Figures

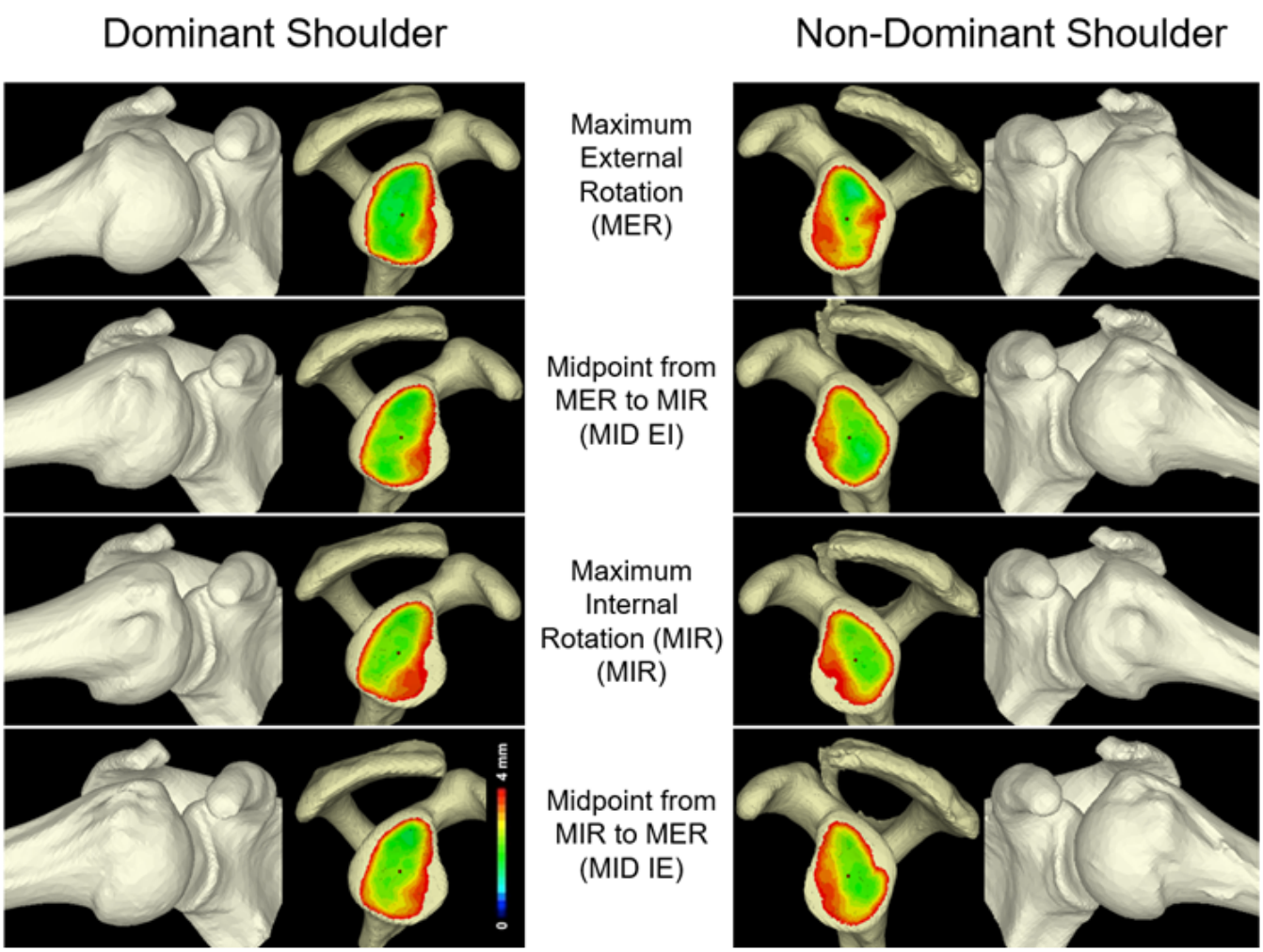

Figure 1

Changes in glenohumeral contact area during simulated pitching motion. Black dot, center of glenohumeral contact area; MER, maximum external rotation; MIR, maximum internal rotation; MID EI, midpoint from MER to MIR; MID IE, midpoint from MIR to MER.

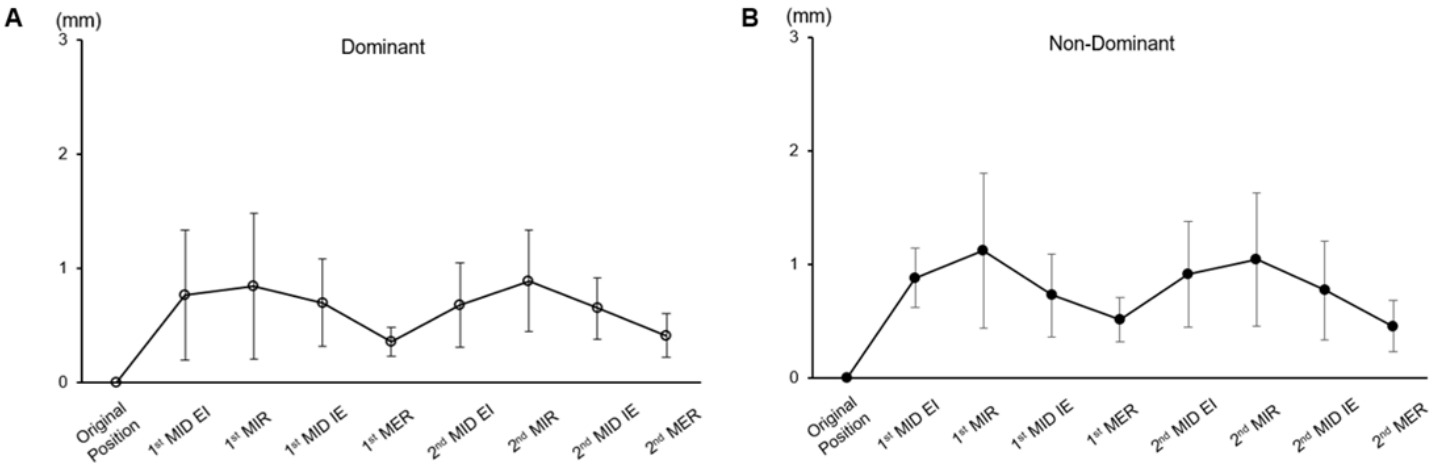

Figure 2

Distance of glenoid contact area centroid from original position to each position. A: dominant shoulder, B: non-dominant shoulder. MER; Maximum external rotation. MIR; Maximum internal rotation. MID EI; Midpoint from MER to MIR, MID IE; Midpoint from MIR to MER.

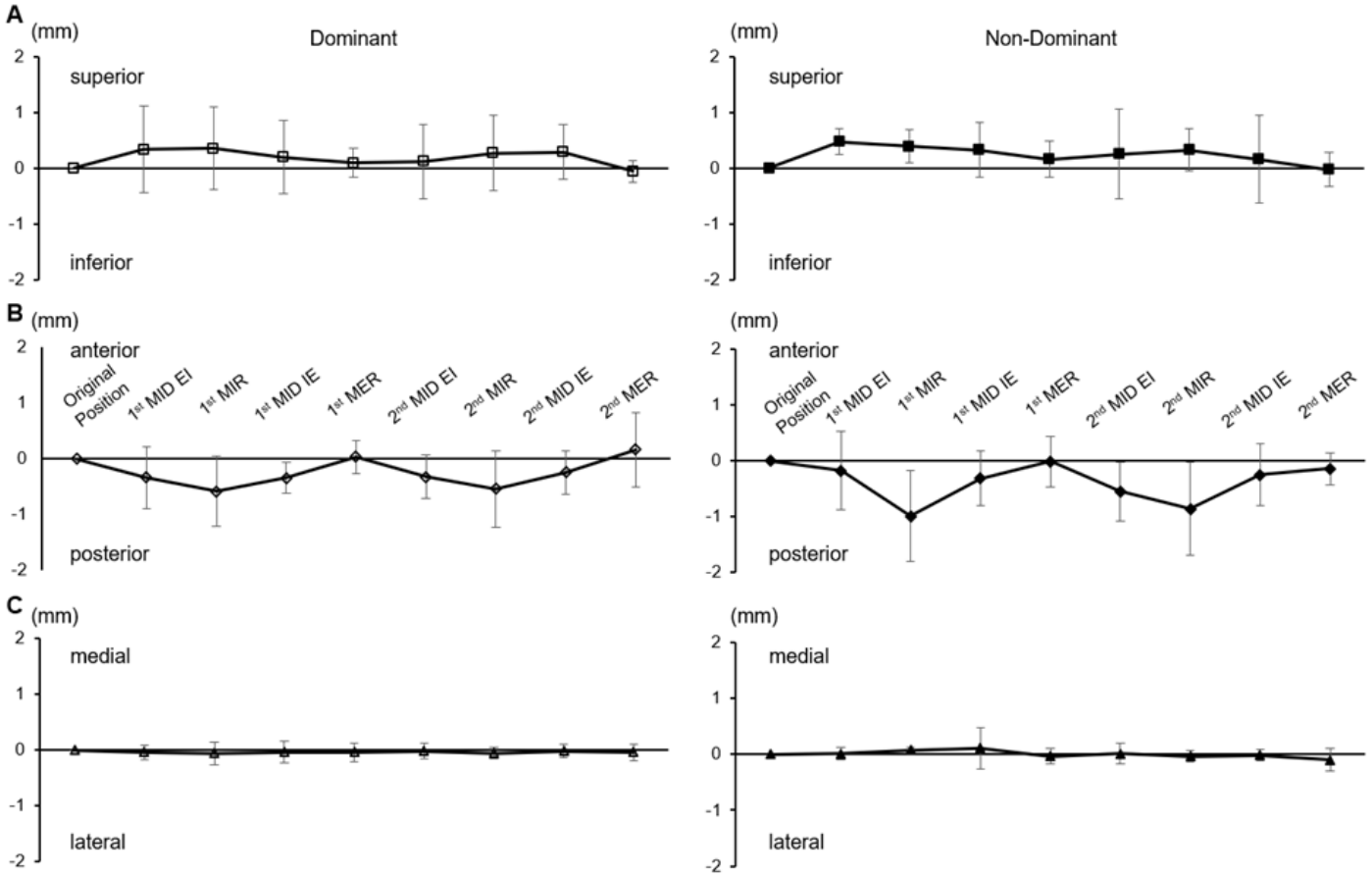

Figure 3

Translation of the center of glenoid contact area from the original position to all other positions. A: superior/inferior directions, B: anterior/posterior directions, C: medial/lateral directions. MER, maximum external rotation; MIR, maximum internal rotation; MID EI, midpoint from MER to MIR; MID IE, midpoint from MIR to MER.

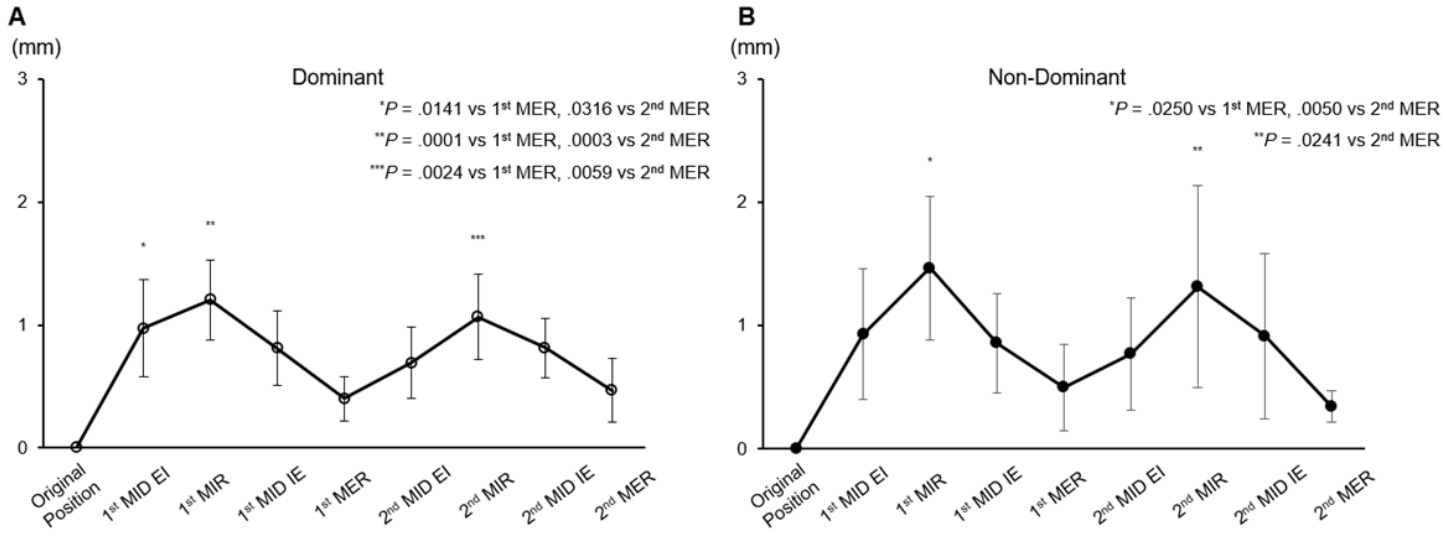

Figure 4

Distance of the center of humeral head from the original position to all other positions. A: dominant shoulder, B: non-dominant shoulder. MER, maximum external rotation; MIR, maximum internal rotation; MID EI, midpoint from MER to MIR; MID IE, midpoint from MIR to MER.

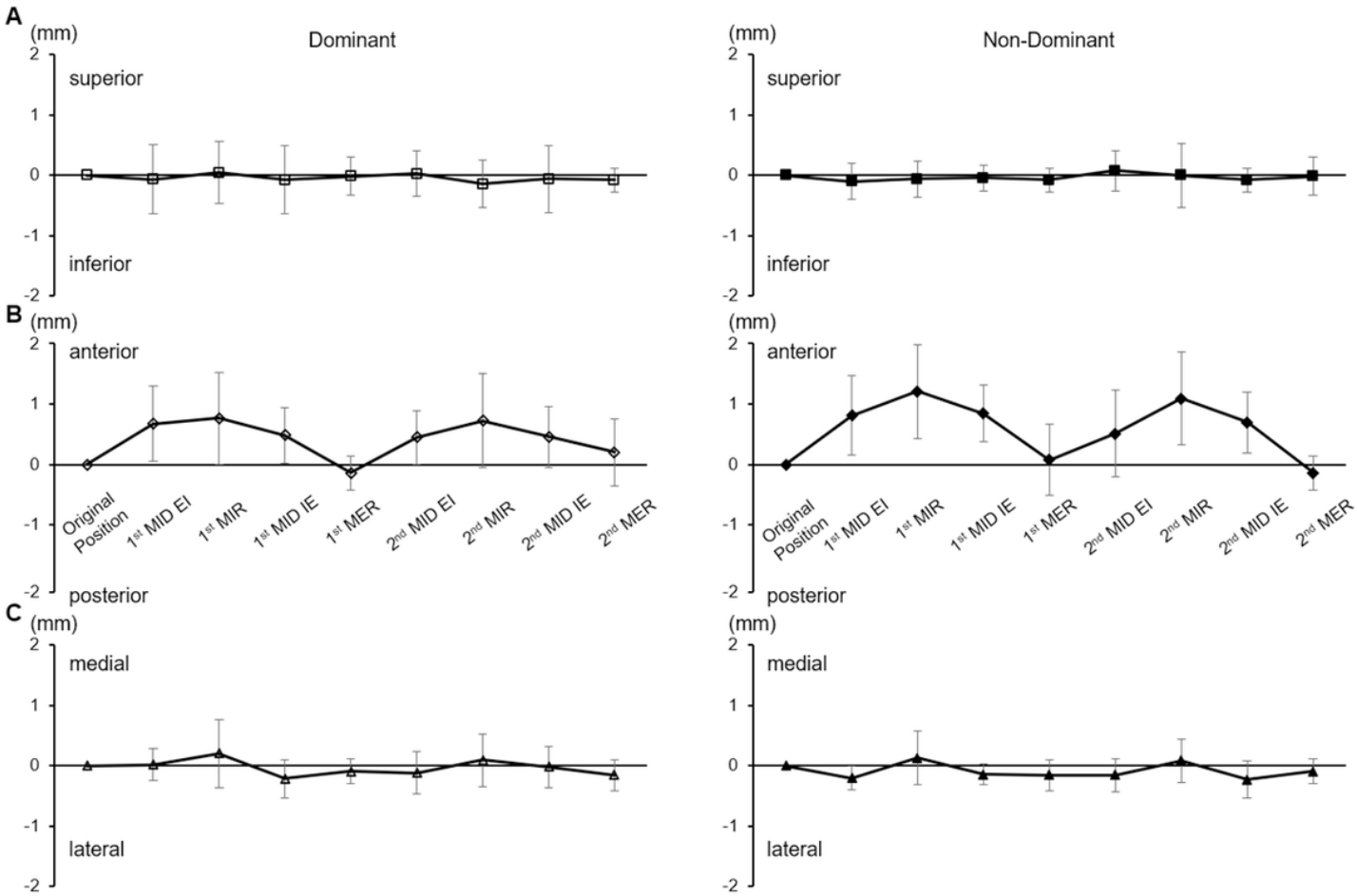

Figure 5

Translation of the center of humeral head from the original position to all other positions. A: superior/inferior directions. B: anterior/posterior directions. C: medial/lateral directions. MER, maximum external rotation; MIR, maximum internal rotation; MID EI, midpoint from MER to MIR; MID IE, midpoint from MIR to MER.

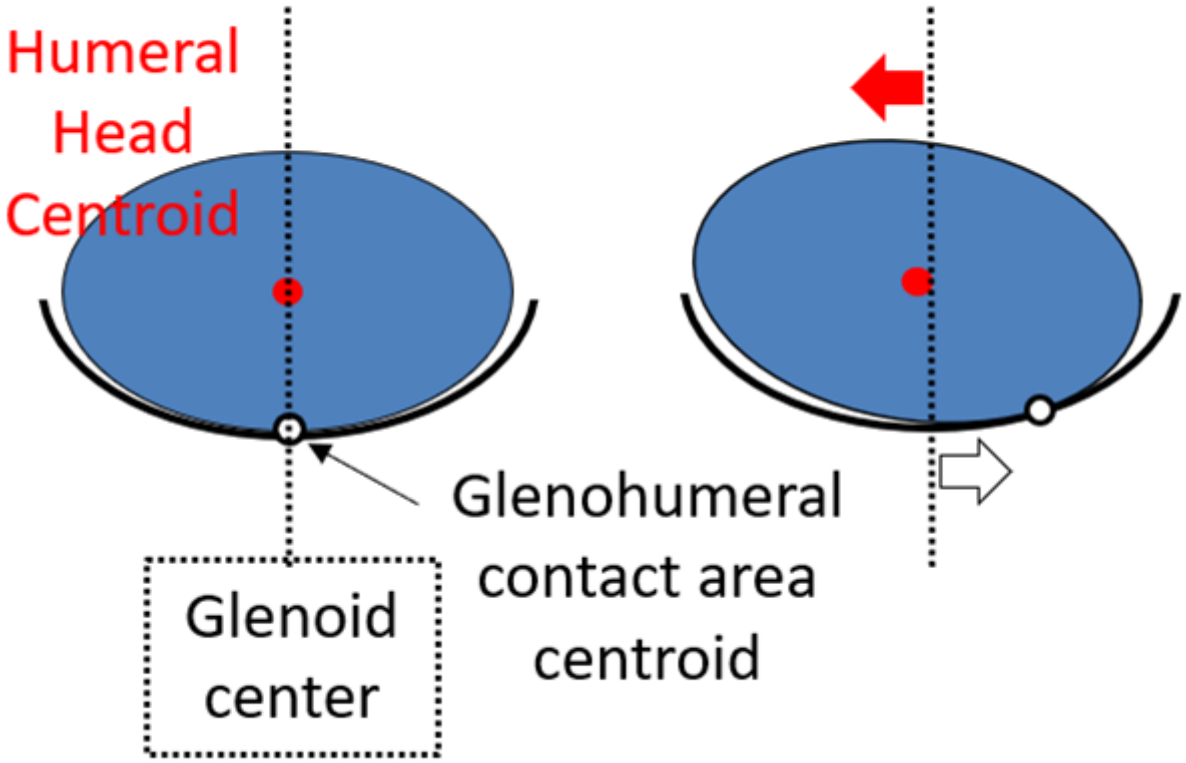

Figure 6

Influence of oblateness of humeral head on translation of the center of glenohumeral contact area and the center of humeral head during shoulder rotation.

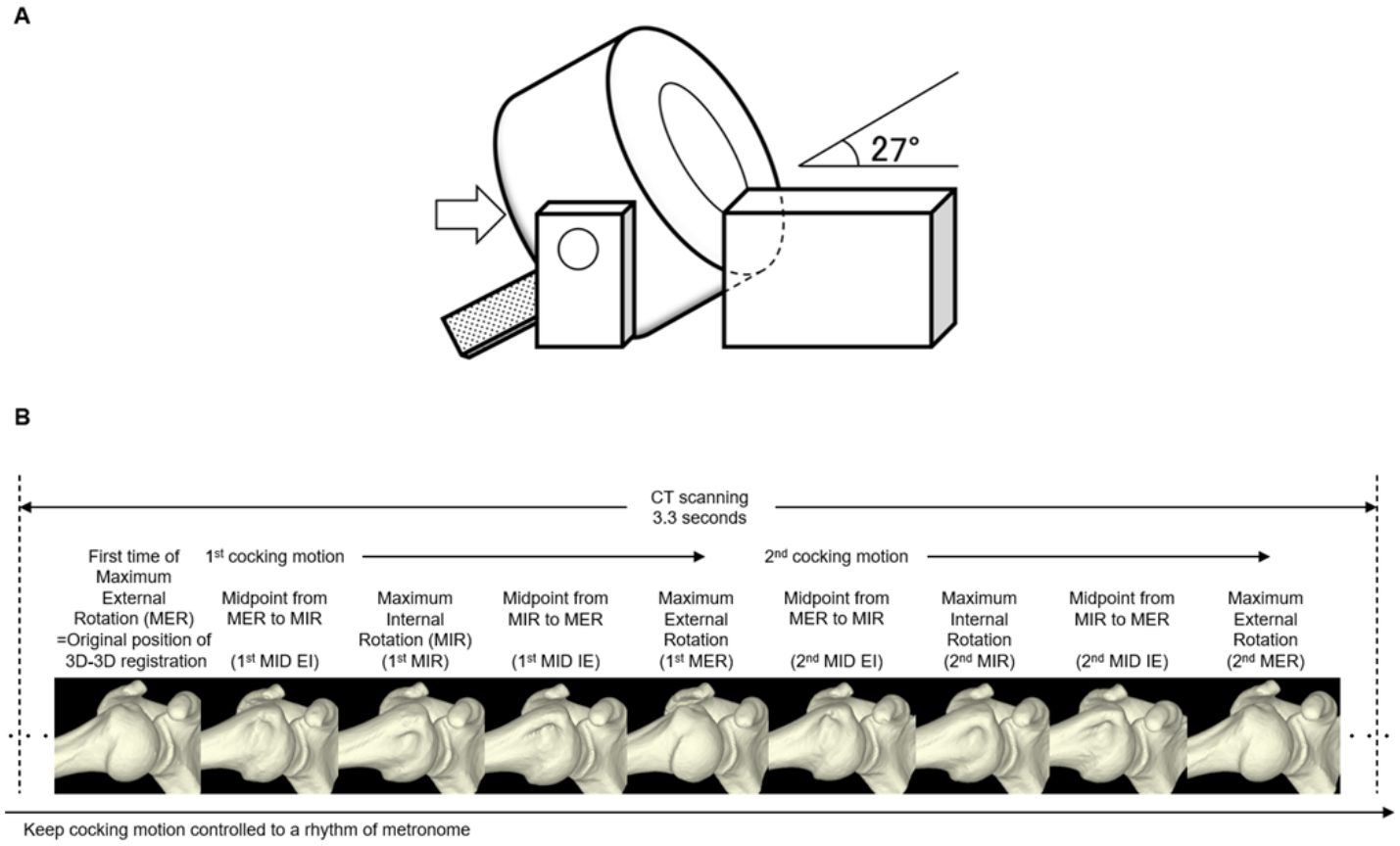

Figure 7

4D CT scanning of the shoulder joint during simulated pitching motion. A: 4D CT image acquisition, B: definition of each shoulder position. MER, maximum external rotation; MIR, maximum internal rotation; MID EI, midpoint from MER to MIR; MID IE, midpoint from MIR to MER.

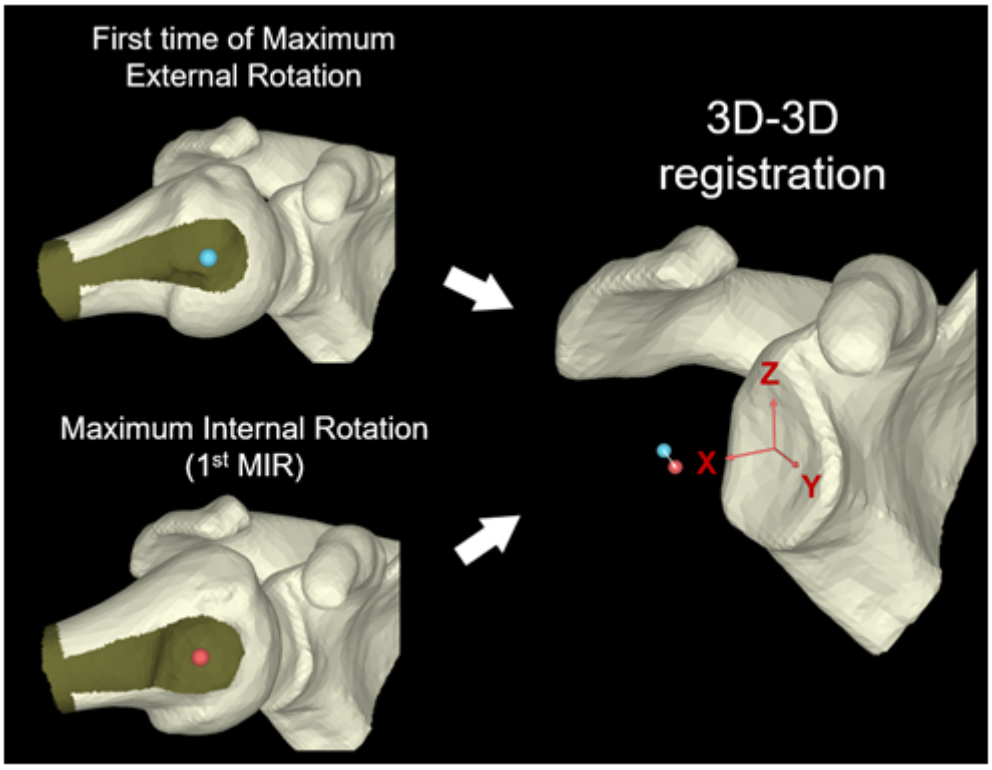

Figure 8

Translation of center of humeral head (CHH). Blue sphere; CHH at the original position, Red sphere; CHH at the first maximum internal rotation.

Supplementary Files

This is a list of supplementary files associated with this preprint. Click to download.

- 202103304DCTTable1.pdf